Investigation of the Antimicrobial Activity and Hematological Pattern of Nano-Chitosan and its Developed Nano-Copper Composite

Somia Ahmed
Imam Abdulrahman Bin Faisal University
Hadeer Mohamed (hiibrahim@iau.edu.sa)
Imam Abdulrahman Bin Faisal University
Abeer Al-Subaie
Imam Abdulrahman Bin Faisal University
Ahoud Al-Ohali
Imam Abdulrahman Bin Faisal University
Nesrine Mahmoud
Imam Abdulrahman Bin Faisal University

Research Article

Keywords: Cs-CuO, pomegranate peels, biogenic nanoparticles, Cs-NP's

Posted Date: January 21st, 2021

DOI: https://doi.org/10.21203/rs.3.rs-149486/v1

Abstract

Novel synthesized Chitosan-Copper oxide nanocomposite (Cs-CuO) was prepared using pomegranate peels extract as green precipitating agents to improve the biological activity of Cs-NP's which was synthesized through ionic gelation method. The characterization of biogenic nanoparticles Cs-NP's and Cs-CuO-NP's were investigated structurally, morphologically to determine the full descriptive features of those nanoparticles. Antimicrobial activity was tested for both Cs-NP's and Cs-CuO-NP's via Minimum inhibition concentration and zone analysis against fungus, gram positive and gram negative. The results of the antimicrobial test showed high sensitivity of Cs-CuO-NP's to all microorganisms that are tested in concentration less than 20 mg/ml while the sensitivity of Cs-NP's against all microorganisms under test started from a concentration of 20 mg/ml to 40 mg/ml except for the C.albicans species. Hematological activity was also tested in via measuring the RBCs, platelets count and clotting time against healthy, diabetic and hypercholesterolic blood samples. Measurement showed a decrease in RBCs and platelets count by adding Cs-NP’s or Cs-CuO-NP's to the three blood samples. Cs-NP’s success to decrease the clotting time for healthy and diabetic blood acting as a procoagulant agent, while adding biogenic CuO-NP’s to Cs-NP’s increased clotting time considering as an anticoagulant agent for hyperchloesterolic blood samples.

1. Introduction

Throughout the history, wound healing has been a crucial challenge facing all wound care researchers in the medical field. Wound healing is a process of repairing tissue integrity through a series of phases including hemostasis, inflammation, proliferation, and remodeling [1]. The initial stage which is the initiation of coagulation cascade to prevent excess blood loss leading to platelet accumulation and fibrin clot formation is known as Haemostasis. Halting in any healing stage leads to chronic wound susceptible to anincrease in microbial infections, large exudates, and necrosis in tissues due to an upsurge in pus cells number[2][3]. Therefore, recent research has focused on improving wound dressing materials specifically those that originated from natural polymers to becoming interactive and bioactive materials.

Chitosan is the most naturally abundant biopolymer and the second most abundant polymer coming after cellulose [4]–[6]. Chitosan being polycationic at acidic media (pH < 6) allows it to interact easily with negative charged molecules, such as phospholipids, anionic polysaccharides, proteins and fatty acids. Nonetheless, chitosan may also chelates metal ions selectively such as copper, iron, cadmium and magnesium [7]. Chitosan plays an important role in the regeneration of the wounded area via fibroblast proliferation and precence of glucosamine which enhances earlier synthesis of hyaluronic acid to acclerattethe healing process with minimal scarring [8], it also helps in revascularization, and plays a role in protecting against atherosclerosis [9]. Additionally, chitosan is able to control inflammatory mediators to accelerate the healing process [9].

Chitosan based nanoparticles, being versatile, nontoxic, biocompatible and biodegradable snatched the attention of researchers in the biomedical field [10][11]. Interests in improving nano chitosan properties

via chemical modification have been growing rapidly [11]. Chitosan chemical modification is of great interest because it can retain its basic skeleton, which in turn keeps its physicochemical and biological properties [10].

Chitosan with various modifications [8][9][12] and several reactive functional sites has shown high activity as an innate antibacterial agent specially when mixed with metallic nanoparticles. Copper is one of the metallic nanoparticles, which is a vital element, in trace amounts, that facilitates the activity of a variety of enzymes, and it also helps in skin regeneration, wound healing process, and angiogenesis [12]. Although, some previous studies showed restraints concerning copper due to its toxicity which is known to emerge from the production of oxy-radicals which initiates the formation of ROS resulting in oxidative stress [12][13]. However, the literature revealed that the hybridization of Copper with chitosan reduces the toxicity level [14]. Also it was repoted that nano Cu and CuO are considered as effective antibacterial agents[14][15][16], According to the literature, chemical reduction method is a facile process for the synthesis of NP's using biopolymeric materials [17] in achieving a better substantial bacteriostatic/bactericidal property.

Copper/Copper oxide nanoparticles (Cu/CuO-NP's) were biologically synthesized using different plant extracts as reducing agent as well as capping agent. These plant extracts have promising advantages towards enhancing biological activity of the CuO-NP's. Pomegranate peel is rich with significant amounts of polyphenols, that is, phenolic acids, such as ellagic and gallic acid, flavonoids and Tannis [18], [19] which are effective as antimicrobials, antianxiety, antidepressant, antiproliferative, antitumor, antioxidant agents [20][21] anticoagulants, antiplatelets, and antianemic agents [22][23] and play a preventive role in cardiovascular diseases by inhibiting coagulation and thrombus [24]. Also it was proved that it had vital role in treating the blood vessels and heart, such as heart attack, atherosclerosis, and high cholesterol. It is also used for conditions of the some digestive tract diseases, including diarrhoea and intestinal parasites[25]. Anticoagulant, antiplatelet, and hypofibrinogenemic effects of *P. granatum* may be due to impaired activity of thrombin predominantly by TAT complex and PC [26].

The aim of this work is to synthesize a hybrid bioactive nanocomposite from marine based polymer, which provides antibacterial efficiency, playing a pivotal role in the healing process.

2. Results And Discussion

2.1 Structural and morphological characterization

2.1.1. FTIR Analysis

FTIR of biogenic synthesized Cs-NP's and Cs-CuO-nanocomposites were investigated (Figure 1) with the data of characteristic peaks were listed in Table (1):

Table 1
FTIR bands of Cs-NP's and Cs-CuO-nanocomposite

Cs-NP's	
Bands locations (cm^{-1})	The indication of bands
3550 – 3000	Overlapping between N – H and –OH starching[32][33]
1638	Carbonyl group of amides[32][33]
1532	N – H bending vibration of amide[32][33]
1382	-CH_3Symmetricaldeformation mode of amide group [33]
1100	Starching vibration of C – O – C linkages of polysaccharides[32]
1094 and 1021	Skeletal starching vibration of C – O [32]
1222	P=O stretching[32]
Cs-CuO-NP's	
3550-2902	Overlapping between N – H, –OH starching from chitosan[32][33]with –OH of carboxylic acid, phenol or alcohol and C – H starching vibration of aliphatic compound of pomegranate peel[34]
1626	Carbonyl group of amides[33]
1521	N – H bending vibration of amide[32]
1371	-CH_3Symmetricaldeformation mode of amide group [32]
1327	Skeletal vibration of aromatic ring of pomegranatepeel[34]
1094	Skeletal starching vibration of C – O [32][33][34] from both chitosan and pomegranate peel
618	Interaction between chitosan and Cu-NP's [33]

The data listed in table (1) illustrates that the difference in the FT-IR pattern between Cs-NP's and Cs-CuO-NP's is due to the existence of a few peaks belonging to Cs-CuO-NP's at 1327 cm^{-1} which indicate the existence of skeletal vibration of aromatic ring of pomegranate peel; this is besides peaks at 3550- 2902 and 1094 cm^{-1}, which overlap with the peaks of chitosan. On the other hand, the appearance of a peak at 616 cm^{-1} and the shifting in many of the peaks' location clearly refers to the interaction between nano chitosan and CuO [32][33][34][35]. Finally, the data from the above table reveals the formation of hybrid nano-composite between nano-chitosan and copper oxide, capped by pomegranate peel extract residual.

2.1.2. XRD Analysis

XRD analysis describes crystalline structure and assesses the compatibility of each component present in the synthesized composite. Figure 2 shows the XRD patterns of Cs-NP's and Cs-CuO-NP's. The XRD of chitosan nanoparticles (Cs-NP's) had a broad peak at 2θ=25° due to the deformation of the crystalline regions which lead to ionic crosslinking with tripolyphosphate, increasing the packing of chitosan chains resulting in the formation of amorphous chitosan nanoparticles [36]. This could be ascribed as a result of the substitution of hydroxyl and amino groups due to the deformation of the hydrogen bond in the original chitosan chain [37], which efficiently breakdown the regularity of the of the main chitosan chains packing.

Cs-CuO-NP's show crystalline peaks of mixed phases of CuO and metallic Cu. CuO patterns were recorded at 2θ= 32.7°, 35.3°, 38.7°, 48.0°, and 53.2° which was assigned to (−110), (002), (111), (−202), and (020) reflections, respectively[38] of the monoclinic structure of the CuO phase, in agreement with JCPDS card No. 45-0937 with lattice parameters a = 0.4685 nm, b = 0.3889nm, and c = 0.513 nm, along with angles α = γ = 90° and β = 99.549°. Cu patterns were detected at 2θ = 43.6° and 50.8° which were assigned to (1 1 1) and (2 0 0) of FCC copper nanopowderin agreement with JCPDS 04–0836 [39].

Some impure peaks from capping nanocmposites with pomegranate peels were detected superimposed on the broad amorphous peak of the chitosan matrix [40] observed at 2θ=25.8°, 28.5°, 40.5° and 49.47° (JCPDS 77-2176 and 87-0730), which revealed the presence of the K_2O and K_2CO_3; while the intense peaks at 2θ=29.0°, 30.3°, 39.4°, 47.5, 32.54, and 53.03 (JCPDS 47-1743 and 37-1497) were attributed to CaO and $CaCO_3$, and the peaks at 2θ=25.1°, 33.0°, 42.05°, 50.3°, and 51.40° were attributed to SiO_2, Fe_2O_3, P_2O_5, carbon and sulfur (JCPDS 41-1413, 33-0664, 5-0488, 75-1621 and 34-0941). Another peak was also observed at 2θ=17.92º due to metal hydroxides.

2.1.3. SEM and TEM

Surface morphology, size and elemental structure of synthesized Cs-NPs and Cs-CuO nanocomposite were analyzed using SEM, TEM and EDX. Figures 3a and 3b revealed a clustered, homogenous distribution of an exemplary spherical shape of nanoparticles with narrow particle size distribution ranging from 20 to 30 nm. Figure 3c confirmed that these nanoparticles mainly composed of C, N, O and P. The SEM image (Figure 3d) showed two types of nanoparticles aggregate on the surface with particle size ranging from of 18 to 40 nm. Figure 3f confirmed that these spherical shape particles are CuO NPs embedded on a chitosan matrix as shown in Figure 3e.

2.2. Antimicrobial Test

The antimicrobial activity of the Cs-NP's and the Cs-CuO-NP's were investigated by the inhibition zone assay against fungus (C. neoformans & C.albicans) , gram positive (Staph. aureus & B. subtilis) and

gram negative (P. aeruginosa & E. coli) , respectively. Although both synthesized samples exhibited wide range of antimicrobial activity but, the biosynthesized Cs-CuO-NP's are expected to possess higher antimicrobial sensitivity than Cs-NP's due to the synergistic effect of chitosan, CuO and pomegranate peel extract. Two significant observations are clear from the results in Figure 4. First, the concentration of both samples examined (10 mg/ml and 50 mg/ml) affects the diameter of inhibition zones growth and their antimicrobial efficiency. Second, the diameter of the growth inhibition zone increases upon loading of CuO-NP's and due to the capping effect of the green extract used in preparation of the hybrid composite. It was found that the all microorganisms tested could grow under the 10 mg/ml of chitosan NP's except C. neoformans which was affected by Cs-NP's, whereas similar concentration of chitosan/CuO nanocomposites inhibit the growth of C. neoformans, B. subtilis and E. coli with diameter 22mm, 13mm and 10mm respectively. The size of the inhibition zone varied according to the type of bacteria and the differences in the cell membrane structure of the three types of bacteria examined .Upon increasing the concentration of Cs-CuO-NP's (50 mg/ml), it implied proficient inhibition in the growth of more species namely Staphylococcus aureus, Pseudomonas aeruginosa and Candida albicans with inhibition zone values of 13mm, 12mm and 11mm respectively: these are considered higher values compared to the values recorded in the literature [41].

It is well established in the literature that chitosan derivatives have been significantly inhibiting the gram-positive bacteria [42], while copper oxide NP showed greater activity against gram negative microorganism which is consistent with the findings in this study.

Pomegranate peel extract which acts as the capping agent (confirmed by XRD) was not randomly selected, but, its high tannins and polyphenolic content has been reported as the key factors for the peel antimicrobial activity. The pomegranate peel extract showed a potent sensitivity towards Gram-positive bacteria [43], which is similar to our results; B. subtilis was more sensitive than S. aureus, followed by E. coli [44] as it could affect the transport of substrates into the cell [45]. Additionally, pomegranate peel extract has significant fungal inhibitory activity. Thus, Cs-CuO-NP's were successfully tailored to merge together the activity of chitosan nanoparticles,CuO, and pomegranate peel capping extract to obtain a broad spectrum antimicrobial novel composite. The activity of the nanoparticles is usually ascribed to their small size enabling them to permeate through the bacterial cell membrane[46]. Besides, the positively charged hybrid Cs-CuO-NP's could block the nutrient intake of the cells due to their interaction with negatively charged lipidic bacterial membrane, and thus reducing both cell growth and viability [47]. It is also worth noting that the efficient antibacterial activity of hybrid Cs-CuO-NP's could be due to reactive oxygen species generation by the nanoparticles attached to the bacterial cells, which in turn provoked an enhancement of intracellular oxidative stress[48]. Presence of CuO nanocrystals in Cs-CuO-NP's improve the antibacterial activity by releasing and diffusing Cu^{2+} ions in the agar medium. These Cu^{2+} ions inducethe production of reactive oxygen species (ROS) such as $HO^{\bullet -}$,$O_2^{\bullet 2-}$, $HO_2^{\bullet -}$ and H_2O_2, which cause cell integrity when interacting with the bacteria cells [49]

Minimum inhibitory concentration MIC is a quantitative method used to analyze antibacterial activity. In the current work, MIC was applied to check the antibacterial and antifungal activity of the two

synthesized samples. The recorded MIC values in Figure 4b support the results from the zone of inhibition test, which shows enhanced activity of the Cs-CuO-NP’s towards boththe gram-negative bacterial strain and the gram-positive bacterial strain compared to Cs-NP’s which was consistent with earlier research.[47].

2.3 Haematological Test

Undoubtedly that RBC’s and platlets play an important role in both thrombosis and hemostasis. RBC’s affect the Rheological blood viscosity and platelet aggregation which enable them to act as a procoagulant and prothrombotic blood component. RBC’s interact with platelets, endothelial cells, and fibrinogen, which inturn leads to their incorporation into the thrombin.

In comparison with control blood samples, a noticeable decrease in mean RBC's and platelets counts was observed by adding Cs-NP's to the blood rather than adding Cs-CuO-NP's as shown in figure 5 a & 5 b. Figure 5a shows that adding Cs-NP's decrease the mean RBC's count by 2.8%, 11.1%, and 6.7% in healthy, diabetic, and hyperchlosterolic blood samples respectively. The same decreasing pattern was observed which is determined to be 1.44%, 3.8%, and 5.0% when adding Cs-CuO-NP's into healthy, diabetic and hyperchlosterolic blood samples respectively. However, adding Cs-NP's leads to a decrease in mean platlets count to 22.4%, 24.4%, and 3.0 % in healthy, diabetic and hyperchlosterolic blood samples respectively, in comparison to 11.0% and 2.7% lesser in platlets count upon adding Cs-CuO-NP's into healthy and diabetic blood samples respectively while it increases the platelets count in hyperchlosterolic blood sample (Figure 5b).

The effects of Cs-NP’s and Cs-CuO-NP’s on the coagulation time of healhy, diabetic and hyperchloesterolic blood samples in vitro were also investigated (Figure 5c). It was shown in Figure 5c that Cs-NP’s are able to decrease clotting time for healthy and diabetic blood samples. An opposite effect was observed in hyperchlosterolic blood sample, while adding CuO capped with P. granaum extract to Cs-NP’s (synthesized nanocomposite) act as anticoagulant by increasing clotting time.

The chitosan nanoparticle (Cs-NP’s) gains hemostatic properties from its net positive charge which depend on the DD and number of pronated amine groups [50]. These amine groups initiate attraction with negatively charged red blood cells and platlets (Figure 5a and 5b) enabling chitosan to build a mesh-like spatial structure, which promoted interaction between chitosan and blood components facilitating formation of blood clotting. Also Cs-NP's is able to gradually depolymerized to release N-acetyl-Dglucosamine, which is transported to cells via glucose receptors and has arole in protecting against atherosclerosis. N-acetyl-D-glucosamine which initiates fibroblast poliferation, aids in providing collagen deposition orders and stimulates increased synthesis of natural hyaluronic acid levels at wound sites. It was proved in a previous study that chitosan with moderate DD nearly 68.36% had the most significant procoagulant effect [51][52]. This is attributed to higher degree of DD had more amino groups and hydroxyl groups in the molecules, which form a stronger hydrogen bonds inside the molecules, leading to

a crystalline structure of chitosan that could hardly interact with blood components to promote coagulation [51].

Adding Copper oxide nanoparticles (nCuO) to Cs-NP’s play a vital role in masking and inhibiting the inflammatory activity of chitosan in addition to enhancing wound healing properties of chitosan [53]. It was proved histologically that nCu are able to stimulate proliferation and migration of fibroblasts. Some copper dependent enzymes help in the synthesis of collagen to facilitate wound healing. It was clearly known that chitosan is polycationic at acidic media so it chelate metallic ions such as Fe, Cu or Mg [54]. This prove that Cu ions chelate chitosan nanoparticles suppressing sites of interaction with RBCs and platlets. This could account for the increasing RBCs and platlets count in Figure 5 a and b.

On the other side, when comparing the results of Cs-NP’s with Cs-CuO-NP’s, it was observed that adding Cs-CuO-NP’s lead to more RBC’s and platlets and clotting time (Figure. 5) , this is due to presence of P. granatum extract as capping agent for synthesized composite. It was suggested in previous work that presence of P. granatum inhibit platlets aggregation due to the presence of anthocyanidins in P. granatum that are responsible to supress cyclooxygenase [55] or may be due to the decrease in fibrinogen level [56]. Increasing clotting time is due to the anti-coagulant effect of P. granatum which inhibit thrombin and intrinsic coagulation factor [57].

This proves that Cs-NP's particles are hemostat, can act as a protrombin or procoagulant while Cs-CuO-NP's are recommended as anti-coagulant.

3. Experimental Work

3.1 Preparation of the Green Extract:

A mass of 40 g of pomegranate peel powder is added into 1L of bidistilled water. The mixture is boiled for 30 minutes, followed by filtration to obtain a clear filtrate. This clear filtrate is kept in the fridge at 4°C and is considered as the plant's extract.

3.2 Chitosan Nanoparticles Synthesis:

The nano-chitosan has been prepared by the ionic gelation method [27], where 0.5g chitosan was dissolved in 50 ml of 1.0% (v/v) acetic acid. Afterwards, 1.0% (w/v) of the trisodium polyphosphate (TPP) was added to the former solution with constant stirring for 1 hour. The produced white precipitate (nano chitosan) was isolated and washed several times with deionized water. Finally the product was dried in an oven overnight at 60 °C.

3.3 Bio-Synthesis of Chitosan-Copper Oxide Nanoparticles:

0.5 gram of chitosan was dissolved in 50 ml of 1.0% acetic acid. By drop wise, 1.0% of TPP was adding to the former solution. Then 50 ml of 1.0M of copper sulphate was added to the mixture of chitosan and TPP, followed by adding 50 ml of plant extract drop wise with constant stirring and heating at 80°C for 1 hour. The resulting nanoparticles were isolated and washed several times with deionized water, and then dried in an oven at 80 °C.

3.4 Characterization

3.4.1. Structural Assessment

Synthesized nanoparticles were examined via Fourier Transform Infrared (FTIR) spectra to investigate the the presence of functional and characteristic groups using a Shimadzu FTIR spectrophotometer. The spectra were carried out at a resolution of 4.0 cm^{-1}. To obtain a reasonable signal to noise ratio, 64 scans were completed. The dried nanoparticles were pressed with KBr and tested [28]. To identify the specific peaks of the Cs-NP's and CuO-NP's, x-ray powder diffractometer using Shimadzu XRD with Cu Kα radiation (λ = 1.5418 Å) at a scanning speed of 0.2 S, was used.

3.4.2. Morphological Characterizations

The morphology and the elemental analysis of the synthesized nanoparticles were performed using SEM (FEI, ISPECT S50, and Czech Republic). SEM was operated at 20 kV with a working distance around 10 mm. The samples were fixed on a metallic stub with double-sided adhesive tape. Images were taken at different magnifications to obtain a better visual inspection, and noting important features of the specimens. For TEM, the synthesized nanoparticles were dispersed in ethanol under sonication for 5 minutes, and deposited onto TEM grids with carbon support film. TEM grids were mounted into the TEM upon evaporation of water in the air at room temperature. The images of the specimens were recorded using TEM, FEI, Morgagni 268, and Czech Republic at 80 kV. Finally, the EDAX analyses were performed using EDX-8000 and , Shemadzu [29][30].

3.5 Antimicrobial Test

Antimicrobial activities of Cs-NP's and Cs-CuO nanocomposites were carried out according to NCCLS recommendations (National Committee for Clinical Laboratory Standards,1993). Inhibition zone primary screening tests were performed by the well diffusion method [31]. Inoculums suspension was prepared from using the tested organisms colonies grown overnight on an agar plate. Chitosan nanoparticles and synthesized nanocomposites were dissolved in DMSO with different concentrations (50, 10, 5, and 2.5 mg/ml). The diameter of the inhibition zone indicating antimicrobial activities were measured after a 24 hours incubation at 37^{o}C. This study investigated Cs-NP's and Cs-CuO-nanocomposites against fungi (*C.*

neoformans and C. albicans), gram-positive (*S. aureus and B. subtilis*) and gram-negative bacteria (*E. coli and P. aeruginosa*).

3.6 Haematological Test

3.6.1. Chitosan Solution Preparation

10 mg/ml of Cs-NP's and Cs-CuO nanocomposites were dissolved in 1% acetic acid separately for under 2 hours, stirring at room temperature.

3.6.2. Blood Collection

10 ml of whole healthy, diabetic and hypercholesterolic blood was collected from the antecubital vein using 21-gauge needles with three-way stop-cocks to minimise tourniquet pressure. The collected blood was aliquoted into three tubes containing 3.8% of sodium citrate anticoagulant tubes for all the studies except for the time blood coagulation. The subject selection was conditional on normal platelet counts for healthy blood, high blood glucose ranged from 180-200 mg/dl for diabetic blood, and LDL cholesterol ranged from 160-180 mg/dl for hypercholesterolic blood.

Ethical approval for the research was obtained by the Institutional Review Board of the Imam AbdulRahman Bin Faisal, Kingdom of Saudi Arabia (Reference number: IRB-2020-03-339). This research was performed in accordance with the Declaration of Protecting Human Research Participants Online Training (PHRP no. 2852904) involving Human Subjects and an informed consent form was also signed by all participants.

3.6.3. Complete Blood Count (CBC)

CBC was carried out on the haematology analyzer CELLTAC to determine haemoglobin level (HGB, g/L), red blood cells count (RBC, count/mm^3) and platelets counts (PLT, count/mm^3). CBC were measured by adding 0.5 ml of Cs-NP's and Cs-CuO nanocomposite solutions into 1.5 ml of each blood sample, aliquoted in 3.8% sodium citrate anticoagulant tubes. The blood incubated in a water bath at 37^oC for 5 minutes, and it was then measured using CELLTAC.

3.6.4. Blood Coagulation Time (BCT)

BCT was measured by adding a solution of 0.5 ml of Cs-NP's and Cs-CuO nanocomposite into 1.5 ml from each blood sample. The blood was incubated in a water bath at 37ºC for 5 minutes, and then the blood coagulation was observed by inclining the tube at 30 second intervals until the blood is clotted.

When the blood flow was not observed up on inclination of the tube at a 90º angle, which indicated blood became coagulant. BCT was measured from the immediately after blood collection until blood coagulation was observed.

Conclusion

Cs-CuO-NP's and Cs-NP's were greenly synthesized and characterized then biological applied to illustrate the following: firstly, the characterization of prepared Cs-CuO-NP's and Cs-NP's found that both biogenic nanoparticles are in spherical shape with particles size around 20- 40 nm. The characterization also provide the formation of Cs-CuO-NP's as hybrid nano–composite from nanochitosan and copper oxide capping with pomegranate peel residual. Secondly, the anti microbial activity inhibition zone test for both Cs-NP's and Cs-CuO-NP's show the superiority of Cs-CuO-NP's as antimicrobial agent over Cs-NP's. The results obtained that Cs-CuO-NP's is highly sensitive to *C. neoformas*, *B. subtilis* and *E. coli* at low concentration 10 mg/ml, in opposite at 10 mg/ml concentration of Cs-NP's aganist all microorganisms, under examination, was effected only on *C. neoformas*. on other hand increasing the concentration of both Cs-NP's and Cs-CuO-NP's to 50 mg/ml increase the sensitivity of Cs-NP's as an antimicrobial agent and also rises by high migraine the ability Cs-CuO-NP's to be lethal for all microorganisms under investigation. While the MIC test clears the role of hybrid composite Cs-CuO-NP's as antimicrobial which found lethal for all microorganisms under test in range of concentration below 20 mg/ml Cs-CuO-NP's, and Cs-NP's found affected only after 20 mg/ml at least for all microorganism except for *C.albicans* species, it was found lethal at 5mg/ml. This comparison between both biogenic nanoparticles proves the importance of hybrid composite of copper and capping agent with nano chitosan in enhances the antimicrobial properties of any biogenic nanoparticals.

Finally, the hematological activity of both Cs-NP's and Cs-CuO- NP's were examined to prove that Cs-NP's particles are hemostat, acts as a protrombin or procoagulant activator used to accelerate blood clotting process for healthy and diabetic patient to prevent Scar. While Cs-CuO-NP's act as anti-coagulant could be used as a coating for coronary stent or drug delivery to prevent arteriosclerosis.

Declarations

Acknowledgment:

This research was chiefly funded by Imam AbdulRuhman Bin Faisal through IAU - 2019 Newly recruited faculty members program supported by Deanship of Scientific Research (DSR) # 2019-224-AMSJ. All authors have the same contribution in this work.

Competing interest:

No

References

1. Velnar,T., Bailey,T. & Smrkolj, V. The Wound Healing Process: An Overview of the Cellular and Molecular Mechanisms. *J. Int. Med. Res.***37**, 1528–1542 (2009).
2. Sen,C. K., Gordillo, G. M., Roy, S., Kirsner, R., Lambert, L., Hunt, T. K., Gottrup, F., Gurtner,G. C. & Longaker, M. T. Human skin wounds : A major and snowballing threat to public health and the economy. *Wound Repair Regen.***17**, 763-771 (2009).
3. Strodtbeck, F. Physiology of wound healing. *Newborn Infant Nurs. Rev.***1**, 43–52 (2001).
4. Chawla, S., Kanatt, S. & Sharma, A. K. Polysaccarides “Chitosan” 1-24 (Springer International Publishing, 2014).
5. Alvarenga, E. Characterization and Properties of Chitosan. *Biotechnol.of Biopolym.***24**, 91-108 (2011).
6. Negm, N. A., Hefni, H. H. H., Abd-elaal, A. A. A., Badr, E. A.& Abou, M. T. H. Advancement on modi fi cation of chitosan biopolymer and its potential applications. *Int. J. Biol. Macromol.***152**, 681–702 (2020).
7. Ahmed, S. & Ikram, S. Achievements in the Life Sciences Chitosan Based Scaffolds and Their Applications in Wound Healing. *ALS*. **10** (1), 27–37 (2016).
8. McCarty, M. F. Glucosamine for wound healing. *Med. Hypotheses*. **47** (4), 273–275 (1996).
9. Ashkani-esfahani, S., Emami, Y., Esmaeilzadeh, E., Bagheri, F. & Namazi, M. R. Glucosamine Enhances Tissue Regeneration in the Process of Wound Healing in Rats as Animal Model : A Stereological Study. *Journal of Cytology & Histology***3**, (4), 3–7 (2012).
10. Mourya V. K. & Inamdar, N. N. Chitosan-modifications and applications : Opportunities galore. *Reactive & Functional Polymers***68**, 1013–1051(2008).
11. Mohammed, M. A., Syeda, J. T. M., Wasan, K. M. & Wasan, E. K. An Overview of Chitosan Nanoparticles and Its Application in Non-Parenteral Drug Delivery. *Pharmaceutics***9**(4), 53 (2017).
12. Mohandas, A., Anisha, B. S., Chennazhi, K. P. & Jayakumar, R. Chitosan–hyaluronic acid/VEGF loaded fibrin nanoparticles composite sponges for enhancing angiogenesis in wounds. *Colloids Surfaces B Biointerfaces***127**, 105–113 (2015).
13. Li, F. *et al.* Analysis of copper nanoparticles toxicity based on a stress-responsive bacterial biosensor array. *Nanoscale***5**, 653-662 (2013).
14. Gopal, A., Kant, V., Gopalakrishnan, A., Tandan, S. K. & Kumar, D. Chitosan-based copper nanocomposite accelerates healing in excision wound model in rats. *Eur. J. Pharmacol.***731**, 8-19 (2014).
15. Borkow, G. *et al.* Molecular mechanisms of enhanced wound healing by copper oxide-impregnated dressings. *Wound Repair Regen.***18**, 266–275 (2010).
16. Figiela, M., Wysokowski, M., Galinski, M., Jesionowski, T. & Stepniak, I. Synthesis and characterization of novel copper oxide-chitosan nanocomposites for non-enzymatic glucose sensing. *Sensors Actuators B Chem.***272,** 296–307 (2018).

17. Farhoudian, S., Yadollahi, M. & Namazi, H. Facile synthesis of antibacterial chitosan/CuO bio-nanocomposite hydrogel beads. *Int. J. Biol. Macromol.***82**, 837–843 (2016).
18. Nijveldt, R., Nood, E., Hoorn, D., Boelens, P., Norren, K. & Leeuwen, P. Flavonoids: A review of probable mechanisms of action and potential applications. *Am. J. Clin. Nutr.***74**, 418–425 (2001).
19. Seeram N. P., *et al.* In vitro antiproliferative, apoptotic and antioxidant activities of punicalagin, ellagic acid and a total pomegranate tannin extract are enhanced in combination with other polyphenols as found in pomegranate juice. *J. Nutr. Biochem.***16** (6), 360–367 (2005).
20. Ismail, T., Sestili, P. & Akhtar, S. Pomegranate peel and fruit extracts: A review of potential anti-inflammatory and anti-infective effects. *J. Ethnopharmacol.***143** (2), 397–405 (2012).
21. Riaz A. & Khan, R. Effect of Punica granatum on behavior in rats. *African J. Pharm. Pharmacol.***8**, 1118–1126 (2014).
22. Torres-Urrutia, C., *et al.* Antiplatelet, anticoagulant, and fibrinolytic activity in vitro of extracts from selected fruits and vegetables. *Blood Coagul. Fibrinolysis***22**, 197–205 (2011).
23. Astudillo, L., *et al.* Fractions of aqueous and methanolic extracts from tomato (Solanum lycopersicum L.) present platelet antiaggregant activity. *Blood Coagul. Fibrinolysis***23**, 109–117 (2011).
24. Wang, X., Hsu, M.-Y., Steinbacher, T. E., Monticello, T. M. & Schumacher, W. A. Quantification of platelet composition in experimental venous thrombosis by real-time polymerase chain reaction. *Thromb. Res.***119** (5), 593–600 (2007).
25. Bhowmik, D., Gopinath, H., Kumar, B., Aravind, D. S. G.& Kumar, K. P. Medicinal Uses of Punica Granatum And Its Health Benefits. *J Pharmacog Phytochem***1**, 28–35 (2013).
26. Riaz, A. & Khan, R. Anticoagulant, antiplatelet and antianemic effects of Punica granatum (pomegranate) juice in rabbits. *Blood Coagul. Fibrinolysis***27**, 1 (2016).
27. Farid, M. S., Shariati, A., Badakhshan, A. & Anvaripour, B. Using nano-chitosan for harvesting microalga Nannochloropsis sp.. *Bioresour. Technol.***131**, 555–559 (2013).
28. Abdel-fattah, W. I., Eid, M. M., El-moez, S. I. A., Mohamed, E. & Ali, G. W. Synthesis of biogenic Ag @ Pd Core-shell nanoparticles having anti-cancer / anti-microbial functions. *Life Sci.***183**, 28–36 (2017).
29. Gabr, D. G. Significance of Fruit and Seed Coat Morphology in Taxonomy and Identification for Some Species of Brassicaceae. *American Journal of Plant Sciences***9,** 380–402 (2018).
30. Mohamed, H. H. & Mohamed, S. K. Rutile TiO_2 nanorods / MWCNT composites for enhanced simultaneous photocatalytic oxidation of organic dyes and reduction of metal ions Rutile TiO_2 nanorods / MWCNT composites for enhanced simultaneous photocatalytic oxidation of organic dyes and reduction of metal ions. *Materials Research Express***5** (1), 1–9 (2018).
31. Chengappa, M. M. “35 - Antimicrobial Agents and Susceptibility Testing,” in *Diagnostic Procedure in Veterinary Bacteriology and Mycology (Fifth Edition)*, Fifth Edition., G. R. Carter and J. R. Cole, Eds. San Diego: Academic Press, 479–492 (1990).

32. Manikandan, A. & Sathiyabama, M. Green Synthesis of Copper-Chitosan Nanoparticles and Study of its Antibacterial Activity. *Journal of Nanomedicine & Nanotechnology***6** (1), 1–5 (2015).
33. Sivakami, M. S., Gomathi, T., Venkatesan, J., Jeong, H., Kim, S. & Sudha, P. N. International Journal of Biological Macromolecules Preparation and characterization of nano chitosan for treatment wastewaters. *Int. J. Biol. Macromol.***57**, 204–212 (2013).
34. Mahmoud, N. M. R., Mohamed, H. I., Ahmed, S. B. & Akhtar, S. Efficient biosynthesis of CuO nanoparticles with potential cytotoxic activity. *Chem. Pap.*, **74** (9), 2825–2835 (2020).
35. Joseph, D., Cruz-romero, M., Collins, T., Cummins, E., Kerry, J. P. & Morris, M. A. Food Hydrocolloids Synthesis of monodisperse chitosan nanoparticles. *Food Hydrocoll.***83**, 355–364 (2018).
36. Martínez-Camacho, A. P., *et al.* Chitosan composite films: Thermal, structural, mechanical and antifungal properties. *Carbohydr. Polym.***82** (2), 305–315 (2010).
37. Raut, A. R. & Khairkar, S.R. Study of Chitosan crosslinked with glutaraldeyde as biocomposite material. *World Journal of Pharmacetical Research***3** (9), 523-532 (2014).
38. Jhansi, K., Chandralingam, S., Reddy, N., Suvarna, P., Chinthakuntla, D. & Rao, K. CuO nanoparticles Synthesis and Characterization for Humidity Sensor Application. *J. Nanotechnol. Mater. Sci.***3**, 1–5 (2016).
39. Zhou, R., Wu, X., Hao, X., Zhou, F., Li, H. & Rao, W. Influences of surfactants on the preparation of copper nanoparticles by electron beam irradiation. *Nucl. Instruments Methods Phys. Res. Sect. B Beam Interact. with Mater. Atoms***266** (4), 599–603 (2008).
40. Patil, R. C., Patil, U. P., Jagdale, A. A., Shinde, S. K. & Patil, S. S. Ash of pomegranate peels (APP): A bio - waste. *Res. Chem. Intermed.***46** (7), 3527–3543 (2020).
41. Jayaramudu, T., *et al.* Chitosan capped copper oxide/copper nanoparticles encapsulated microbial resistant nanocomposite films. *Int. J. Biol. Macromol.***128,** 499-508 (2019).
42. Kong, M., Guang, X., Xing, K. & Jin, H. International Journal of Food Microbiology Antimicrobial properties of chitosan and mode of action : A state of the art review. *Int. J. Food Microbiol.***144** (1), 51–63 (2010).
43. Dahham, S., Ali, M. N., Tabassum, H. & Khan, M. Studies on antibacterial and antifungal activity of pomegranate (Punica granatum L.). *Am. Eurasian J. Agric. Environ. Sci.***9**, 273–281 (2010).
44. Al-Zoreky, N. S. Antimicrobial activity of pomegranate (Punica granatum L.) fruit peels. *Int. J. Food Microbiol.***134** (3), 244–248 (2009).
45. Al-Askar, A. In vitro antifungal activity of three Saudi plant extracts against some Phytopathogenic fungi. *J. Plant Prot. Res.***52**, 458–462 (2012).
46. Sondi, I. & Salopek-Sondi, B. Silver nanoparticles as antimicrobial agent: a case study on E. coli as a model for Gram-negative bacteria. *J. Colloid Interface Sci.*, **275** (1), 177–182 (2004).
47. Haldorai, Y. & Shim, J. Multifunctional Chitosan-Copper Oxide Hybrid Material : Photocatalytic and Antibacterial Activities. *International Journal of Photoenergy***2013**, 1-8 (2013).

48. Applerot, G., Lellouche, J., Lipovsky, A., Nitzan, Y. & Lubart, R. Understanding the Antibacterial Mechanism of CuO Nanoparticles : Revealing the Route of Induced Oxidative Stress. *Small* **21**, 3326–3337 (2012).
49. Hassan, M. S., Amna, T., Yang, O.-B., El-Newehy, M. H., Al-Deyab, S. S. & M.-S. Khil. Smart copper oxide nanocrystals: Synthesis, characterization, electrochemical and potent antibacterial activity. *Colloids Surfaces B Biointerfaces* **97**, 201–206 (2012).
50. Phyllis, J. V. E. Æ., Nicolette, H. Æ., Condon, B., Arnold, Æ. J. & Diegelmann, Æ. R. Positively and negatively charged ionic modifications to cellulose assessed as cotton-based protease-lowering and hemostatic wound agents," *Cellulose* **16** (5), 911-921 (2009).
51. Hu, Z., *et al.* Investigation of the Effects of Molecular Parameters on the Hemostatic Properties of Chitosan. *Molecules* **23**, 3147 (2018).
52. Yang, J., Tian, F., Wang, Z., Wang, Q., Zeng, Y. & Chen, S. Effect of Chitosan Molecular Weight and Deacetylation Degree on Hemostasis. *J Biomed Mater Res B Appl Biomater* **84**, 131–137 (2007).
53. Mohandas, A., Deepthi, S., Biswas, R., Jayakumar, R. Chitosan based metallic nanocomposite scaffolds as antimicrobial wound dressings. *Bioactive Materials* **3**, 267-277 (2018)
54. Huang, D., Xu, B., Wu, J., Brookes, P. C. & Xu, J. Adsorption and desorption of phenanthrene by magnetic graphene nanomaterials from water: Roles of pH, heavy metal ions and natural organic matter. *Chem. Eng. J.* **368**, 390–399 (2019).
55. Aviram, M., *et al.* Pomegranate juice consumption reduces oxidative stress, atherogenic modifications to LDL, and platelet aggregation: studies in humans and in atherosclerotic apolipoprotein E-deficient mice 1,2. *Am. J. Clin. Nutr.* **71**, 1062–1076 (2000).
56. Denninger, M., *et al.* ADP-induced platelet aggregation depends on the conformation or availability of the terminal gamma chain sequence of fibrinogen. Study of the reactivity of fibrinogen Paris I. *Blood* **70**, 558–563 (1987).
57. Di Cera, E. Thrombin review. *Mol Aspects Med* **29**, 203–254 (2008)

Figures

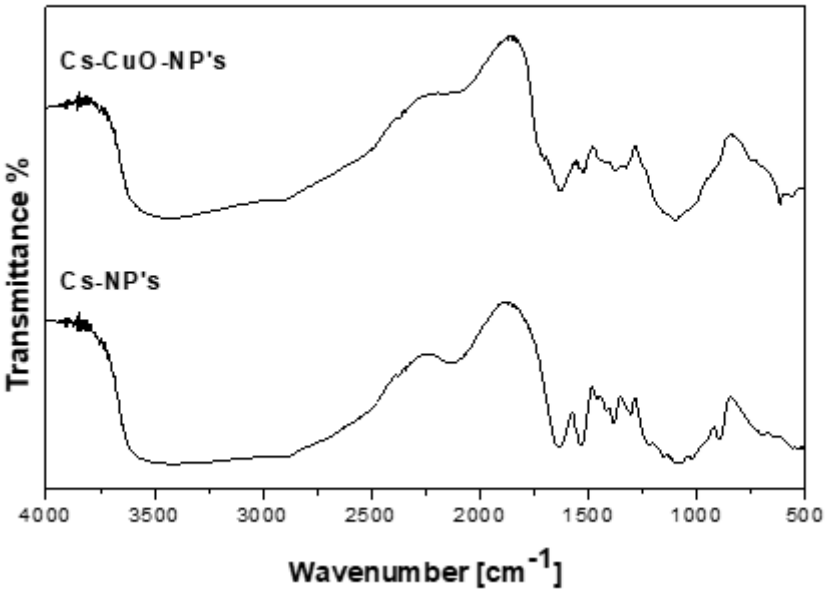

Figure 1

FTIR for (a) Cs-NP's, (b) Cs-CuO-NP's nanocomposite

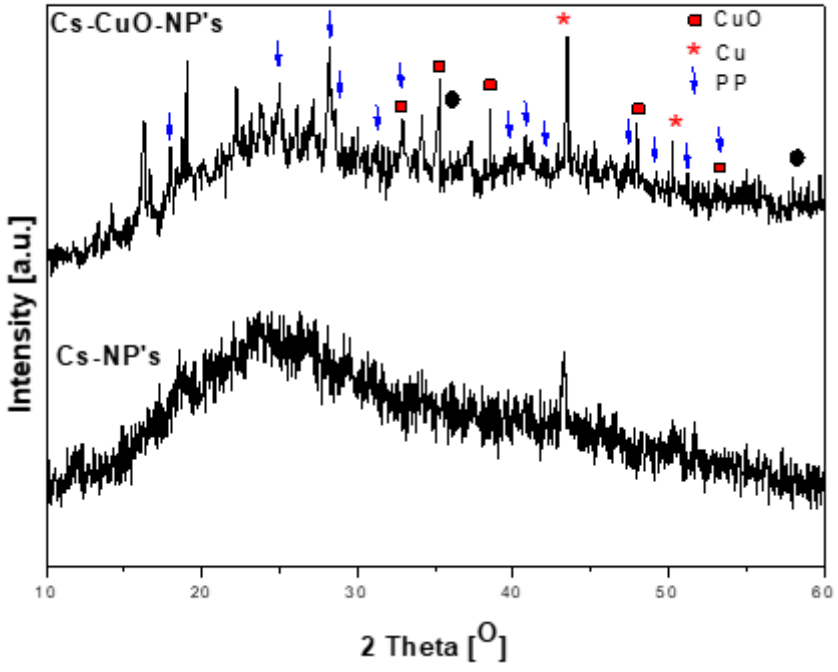

Figure 2

XRD patterns for (a) Cs-NP's , (b) Cs-CuO-NP's

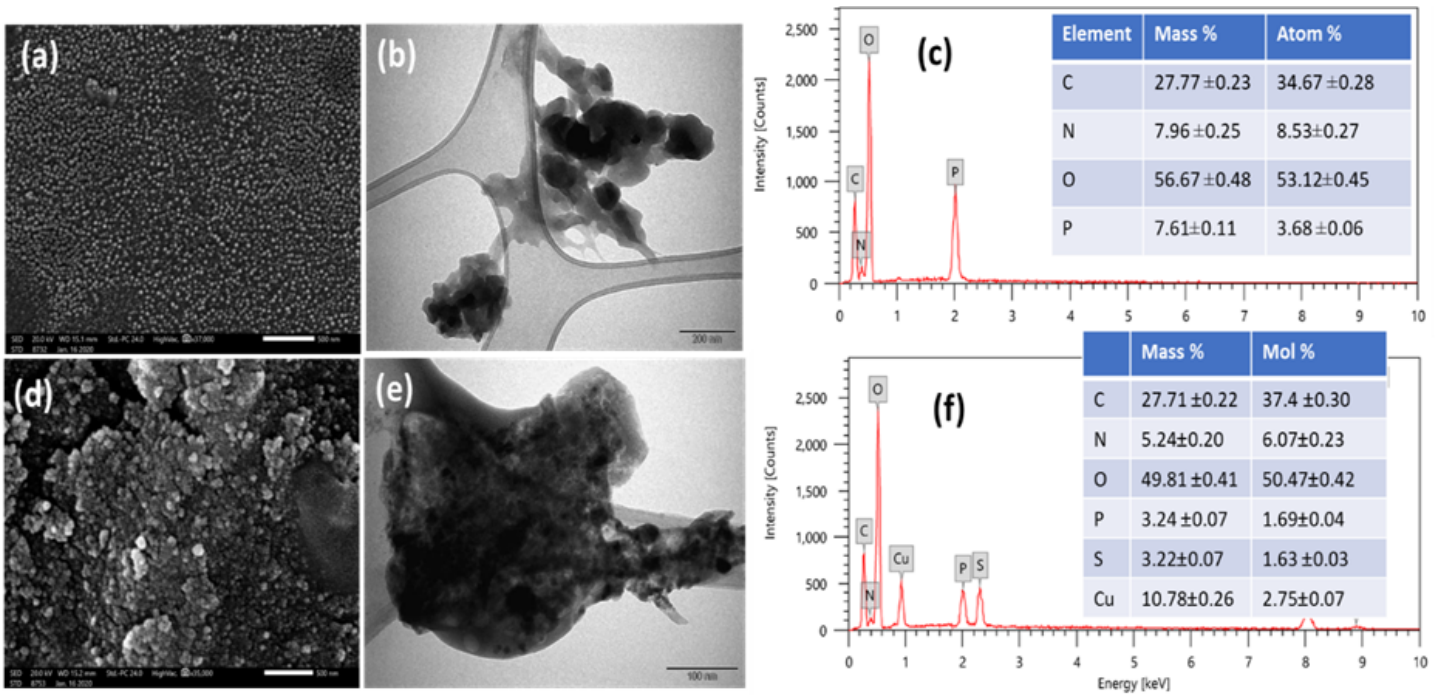

Element	Mass %	Atom %
C	27.77 ±0.23	34.67 ±0.28
N	7.96 ±0.25	8.53±0.27
O	56.67 ±0.48	53.12±0.45
P	7.61±0.11	3.68 ±0.06

	Mass %	Mol %
C	27.71 ±0.22	37.4 ±0.30
N	5.24±0.20	6.07±0.23
O	49.81 ±0.41	50.47±0.42
P	3.24 ±0.07	1.69±0.04
S	3.22±0.07	1.63 ±0.03
Cu	10.78±0.26	2.75±0.07

Figure 3

SEM images of (a) synthesized chitosan NPs, (d) chitosan-CuO nanocomposite; TEM images (b)synthesized chitosan NPs, (e) chitosan-CuO nanocomposite, and edx elemental % (c) synthesized chitosan NPs, (f) chitosan-CuO nanocomposite.

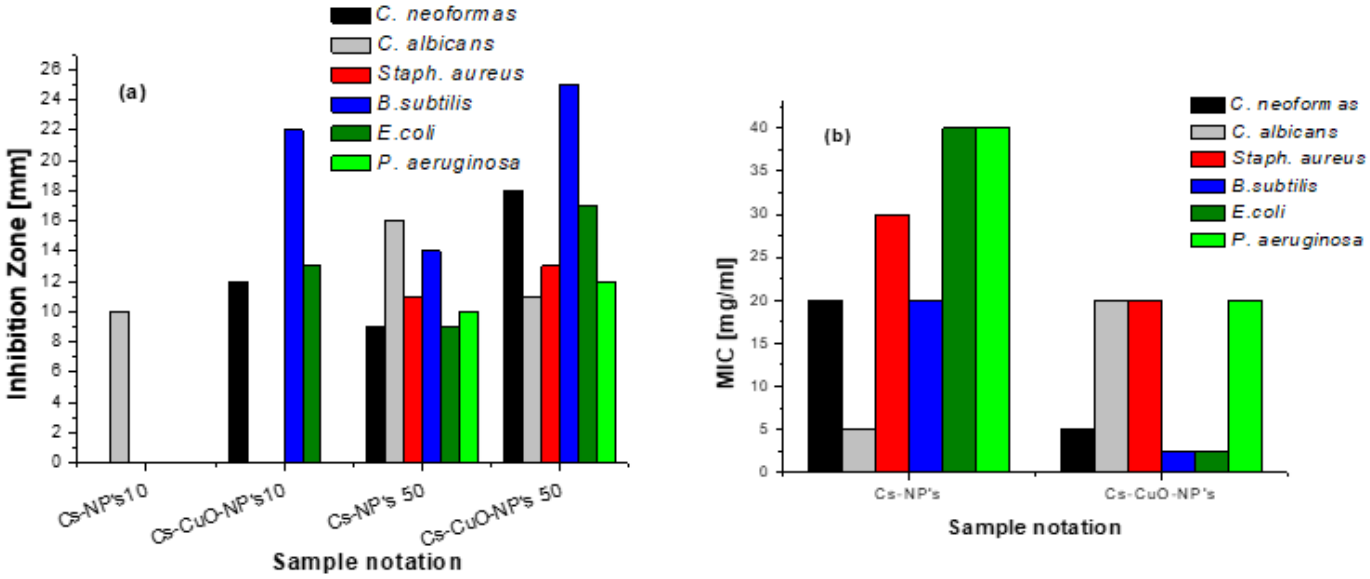

Figure 4

(a) Inhibition zone of Synthesized nanoparticles of Cs-NP's and Cs-CuO-NP's at 10 and 50 mg/ml, (b) Minimum Inhibition Concentrations ofCs-NP's and Cs-CuO-NP's

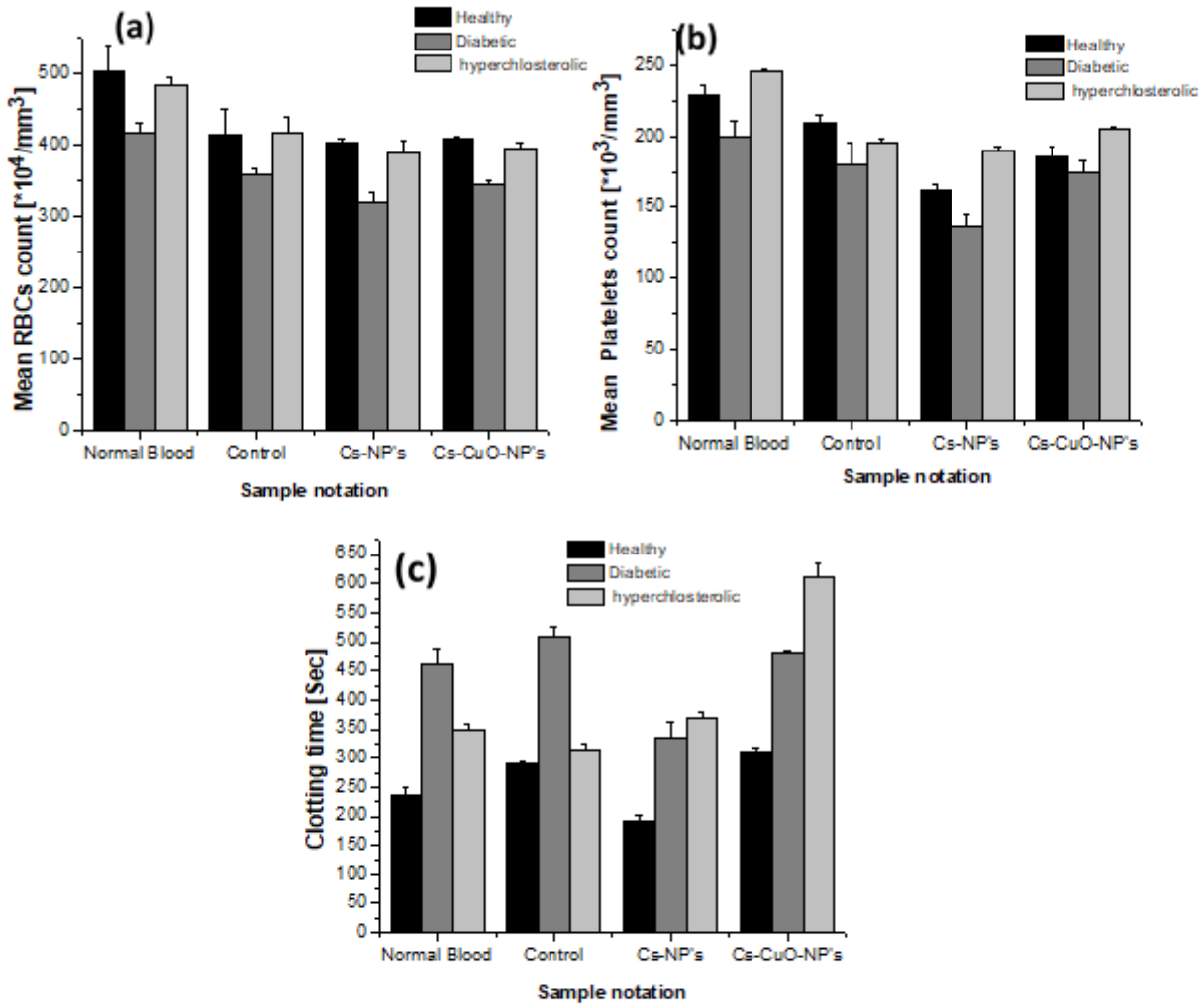

Figure 5

Shows the effect Cs-NP's and Cs-CuO-NP's nanocomposite on (a) Mean RBC's count, (b) mean platlets count and clotting time after adding to healthy, diaebetic and hyperchloesterolic blood samples